A Hydrophobic Surface Based on a Ni-P-PTFE Coating on a Metallic Bipolar Plate

Chien-Hung Lin[1,*], Jia-Ren Lee[2], Pei-Jing Teng[1], Sung-Ying Tsai[3], Hung-Hua Sheu[4], Kung-Hsu Hou[5], Ming-Der Ger[4]

[1] Department of Physics, ROC Military Academy, Feng-Shan, Kaohsiung 830, Taiwan
[2] Department of Physics, National Kaohsiung Normal University, Kaohsiung, Taiwan
[3] Materials and Electro-optics Research Division, Chung-Shan Institute of Science and Technology Tao-Yuan 335, Taiwan, ROC
[4] Department of Chemical and Materials Engineering, National Defense University, Taoyuan, 335 Taiwan
[5] Department of Power Vehicle and Systems Engineering, National Defense University, Taoyuan, 335 Taiwan
[*]E-mail: linhungcma@gmail.com

The performance of 5052 aluminum bipolar plates (BPPs) with surface treatment for proton exchange membrane fuel cell (PEMFC) systems are characterized in this study. The coated bipolar plates are evaluated by the coating composition, contact angle, corrosion resistance, interfacial contact resistance and assembly test. The coated bipolar plate has active water-management ability due to the Ni-P-PTFE (polytetrafluoroethylene) coating layer with low surface energy. The extremely hydrophobic property enhances the contact angle on the solid surface from 72° to 103°. Furthermore, the corrosion resistance of the Ni-P-PTFE and substrate in the simulated environment are 1.02×10^{-6} and 9.22×10^{-4} A/cm^2, respectively. Hence, the substrate with a Ni-P-PTFE coating retains its superior performance after a durability test. The result demonstrates that the whole performance of the PEMFC is directly related to the corrosion resistance and hydrophobic behaviour on 5052 aluminum bipolar plate.

1. INTRODUCTION

The fuel exhaustion and industrial pollution have been important issues during the past decade. The large scale demand for clean energy is increasing dramatically with power vehicle. Proton exchange membrane fuel cell possesses desirable characteristics, such as high conversion efficiency,

low-temperature operation, quick starting and low acoustical pollution [1-4]. Hence, the PEMFC can be extensively applied to power vehicle, power plant and portable equipment [5-8]. The PEMFC lifetime is crucial to entire project as a whole, and the durability and efficiency of proton exchange membrane (PEM) fuel cell must achieve the department of energy's (DOE) target before its commercialization.

The implement revolution of the bipolar plate was discussed in previous study [9]. They suggest the material fabricated into the bipolar plate must be machined easily. In this study, the stainless steel was coated with a thin gold film and demonstrated superior power performance than the graphite. Hence, the investigation indicated that the metal bipolar plate was an ideal substitution for the graphite. The corrosive behaviour of the steel in the PEMFC was observed in simulated environment [10]. The thickness of the oxide film increased around 1 nm of the bipolar plate after the 300h test. Besides, the contact resistance of the bipolar plate increased form 35.5 m$\Omega \cdot$ cm^2 to 174 m$\Omega \cdot$ cm^2. Accordingly, the corrosion behaviour of the steel decreased the whole PEMFC performance severely. This result indicated that the degradation of the PEMFC performance was attributed to the gain of contact resistance between the bipolar plate and the GDL.

Since a metal surface is weak at corrosion resistance, it can still be a potential candidate material to replace expensive graphite for fuel cells in the near further [11-13]. Electrodeposition is also an effective technology to inhibit the metal corrosion in fuel cells. The Ni-P and Ni-Mo-P coating layers were coated on the 6061 aluminum alloy by the electroplating technique [14]. The modified surface was investigated under the simulated environment (0.5M H$_2$SO$_4$ with 2 ppm HF solution). The amorphous structure Ni-Mo-P coating enhanced surface stability which decreased the corrosion current effectively. Additionally, the Ni-Mo-P exhibited the superior conductivity than the substrate. This result proved that the Ni-Mo-P was an ideal bipolar plate candidate material. The carbon-polymer layer was deposited on stainless steel 316L bulk by the spray technology [15]. The coating layer consisted of 45% graphite, 5% carbon black and 50% epoxy binder which enhanced the ICR value and chemical stability in the PEM fuel cell environment. But, the coating layer could not protect the substrate completely from the chemical electrolyte due to large porosity on the surface.

Recently, surface modification of the bipolar plate proved its feasibility that remove interior water and solve the associated water-management issues [16-18]. The various bipolar plates with Ag and Ag-PTFE coating on 316L stainless steel to substitute the graphite bipolar plate were discussed in literature [19]. The Ag-PTFE composite coating layer enhanced the water management ability and corrosion resistance. Hence, the Ag-PTFE composite coating demonstrated hydrophobic behaviour than Ag coating. This result indicated that active water management is another technical issue to the modification of metallic bipolar plate. The metallic bipolar plate surface effect correlated to whole PEMFC performance was discussed in literature [20]. The surface texture of a metallic bipolar plate was treated by mechanical treatment. The interfacial contact resistance depended on the surface roughness of bipolar plate. The interfacial contact area was 2.5 times larger than an untreated substrate as the surface roughness was above 8 μm. The whole performance of the treated PEMFC increases by 17% than the untreated one.

The roughness and contact angle on the bipolar plate were crucial factors of water management for the PEMFC [21]. The contact resistance between the gas diffusion layer (GDL) and the bipolar

plate were discussed in literature [22]. The polytetrafluoroethylene (PTFE) particle was loaded to modify the physical properties of carbon substrates. It demonstrated that the PTFE particle loading influenced the contact resistance between the gas diffusion layer and the bipolar plate significantly. The suitable PTFE particle enhanced the contact angle and conductivity to the component surface.

Hence, strengthen the water management and durability of components will be a trend of metallic bipolar plate development in near future [23]. This paper is concerned with identifying the alternative material (Ni-P and Ni-P-PTFE coating) and assessing their performance in the fuel cell environment.

2. EXPERIMENTS

2.1 Surface treatment

The 5052 aluminum BPPs, designed to single serpentine flow-field, with a geometrical surface area of 25 cm^2 as Fig.1, and the microscopy image at flow channel bottom is inserted in this figure.
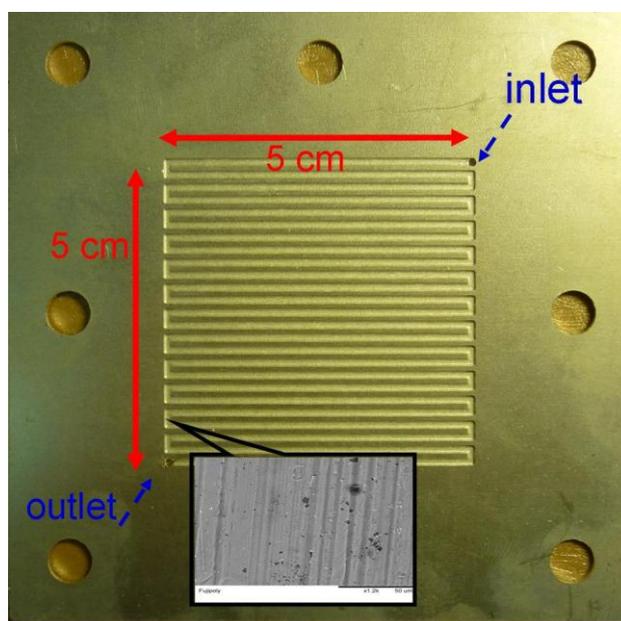
Figure 1. Geometry of 5052 aluminum bipolar plate with a single serpentine flow channel.

The Zn replacement process was executed for the bare aluminum sheet before the electroless deposition. These specimens are degreased by NaOH base solution for 3 min., and cleaned with deionized water. Subsequently, the specimen surface is pickled in nitric acid solution for 3 min and also cleaned by deionized water again. Finally, the specimen is exposed to an electroless solution, and the constant temperature is manipulated at 90℃ for the Ni-P and Ni-P-PTFE coating as Fig.2.
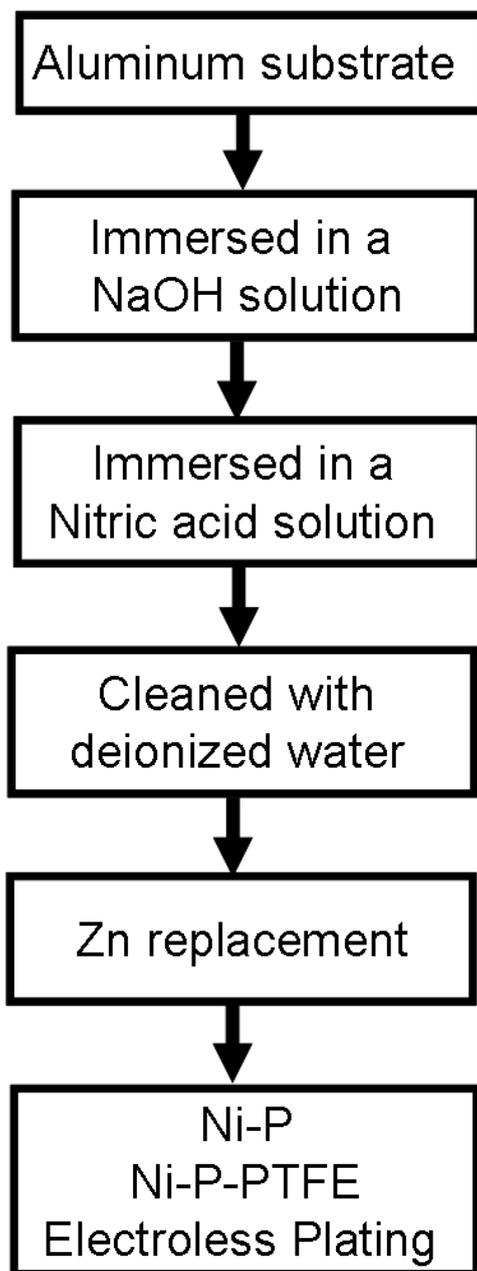
Figure 2. Flow chart of electroless plating on 5052 aluminum sheet.

2.2 Corrosion resistance test

Potentiodynamic polarisation was employed to analyze the corrosion resistance of 5052 aluminum using a Versastat 4 system (AMETEK Inc) with a standard three electrode cell system. In order to investigate the corrosion resistance of 5052 aluminum BPPs in a simulated environment, and specimens with and without coating were exposed to a 0.5 M H_2SO_4 with 2ppm HF solution at room temperature. Meanwhile, the standard three electrode cell system with a platinum electrode (Auxiliary Electrode), Ag/AgCl (Reference Electrode) and the 5052 aluminum BPPS (working electrode) were employed in the polarization test. The stable period (3 min) was executed before the measurement, and

the potential scan started from the open circuit potential. The sweeping potential range and scanning rate were carried out at −1 V to 0.8 V and 0.166m V/sec, respectively.

2.3 Interfacial contact resistance measurement

The experimental setup of interfacial contact resistance is illustrated in Fig.3. The 5052 aluminum sheet was sandwiched between copper plates and two pieces of gas diffusion layer as described in [2, 24]. The actual ohmic loss is composed of the resistance from the bipolar plate and GDL interface, and it was measured as a function of the compaction force. Since the interfacial contact resistance is influenced by the compaction stress, the force ranging from 0 to 300 N/cm^2 was load by a universal compressed machine at this test.
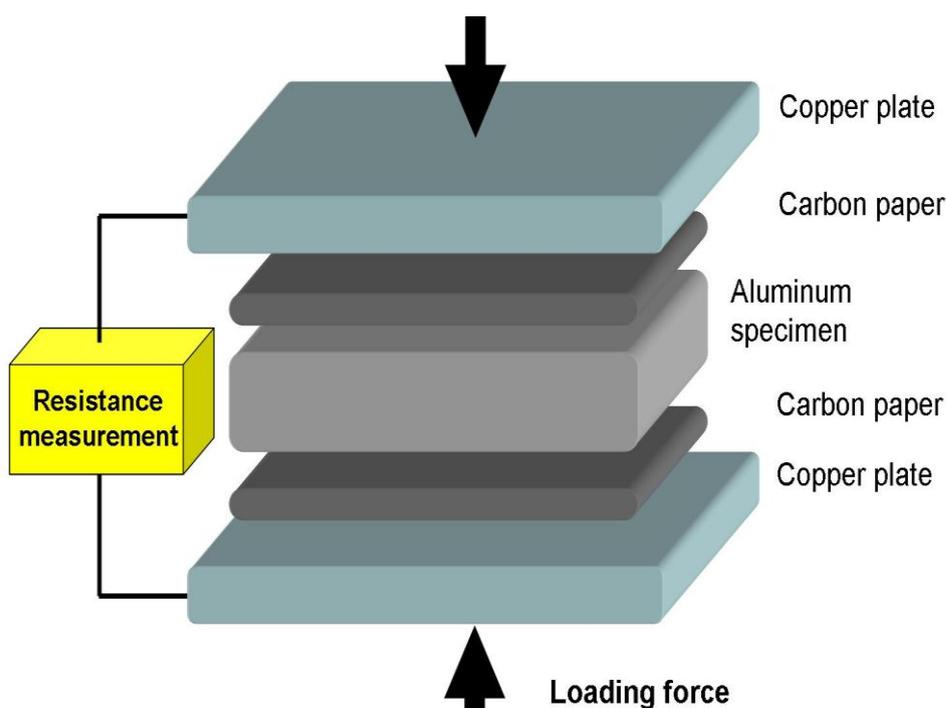
Figure 3. Schematic of the interfacial contact resistance measurement.

2.4 Single cell performance measurement

The main components of single cell are commercial membrane electrode, coated 5052 BPPs, and two pieces of gas diffusion layer. In single cell measurement, the compaction force was loaded as 200 N/cm^2. The membrane electrode composed of Toray paper and Nafion 112 membrane. During the reactive period, the fuel gases are feed into the PEMFC and then the hydrogen gas is oxidized into H$^+$ ions and electrons at anode side. The electrochemical half reaction at the negative side is described as (1). The electrons apart from the hydrogen atoms are forced to flow through the external circuit and provide the work energy.

$$H_2 \rightarrow 2H^+ + 2e^-$$

(1)

Subsequently, hydrogen ions pass through the porous electrode, and then react with the oxygen gas in cathode side. The half reaction at the positive side is described as (2). The fuel cell exists in a discharge mode as reactants are continuously supplied.

$$\frac{1}{2}O_2 + 2e^- + 2H^+ \rightarrow H_2O \qquad\qquad (2)$$

The reactant gas in the anode, cathode side and cell temperature are hydrogen gas (210 sccm), oxygen (140 sccm) and 70℃, respectively. Meanwhile, the measurement is executed in the sweeping potential mode ranging from 0.85 V to 0.3 V. In order to prevent the unstable measurement, the stable period is lasted for 1 hour after the fuel cell supplied with reactant gases.

3. RESULTS AND DISCUSSION

3.1 Composition of surface coating

The microscopy image of the coated layer is observed by a scanning electron microscope 6500F (JEOL Inc). The chemical composition of the interfacial coating is analyzed by energy dispersive X-ray spectroscopy (EDAX) system. As the chemical compositional diagram, the Ni element of the Ni-P and Ni-P-PTFE coatings are 83.89% and 73.98%, respectively [25]. From the SEM image, the electroless Ni-P coating exhibited a smooth, continuous and subcircular structure as previous literature [24, 26]. Furthermore, the latter (Ni-P-PTFE) possesses higher phosphorus content than the former (Ni-P) as Figs. 4-5. Evidently, PTFE particles are embedded on the surface as shown in Fig. 5(a). The modification layer has extremely low surface energy in flow channel to enhance active water management ability due to distributed PTFE particles [19].

(a) SEM image

(b) EDS compositional analysis.
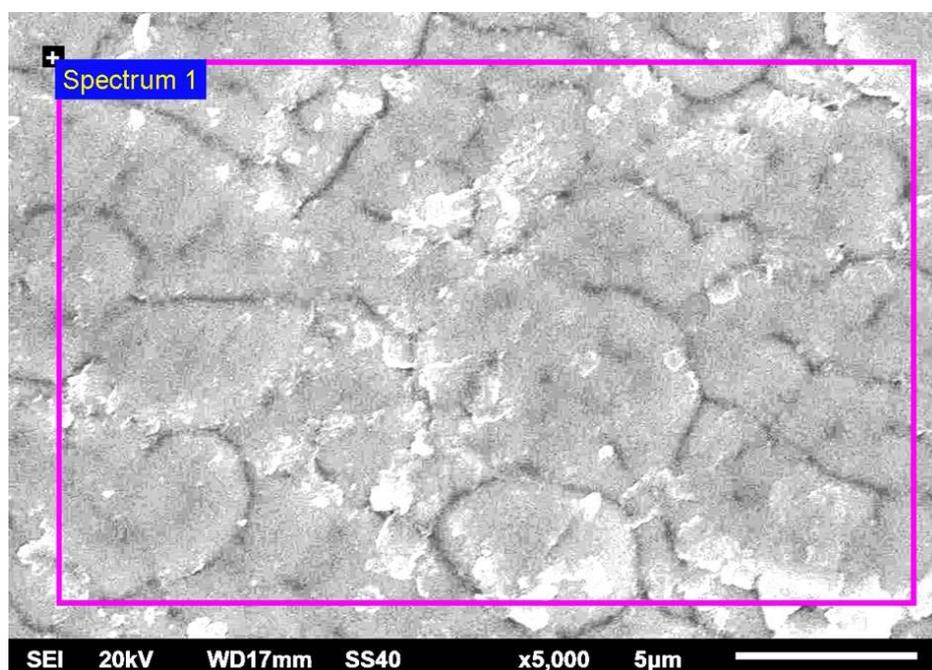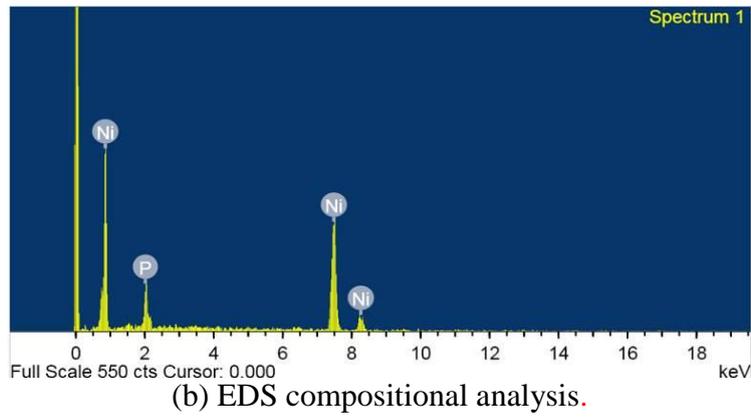
Figure 4. Characterized 5052 aluminun surface subjected to Ni-P electroless coating.

(a) SEM image

(b) EDS compositional analysis.
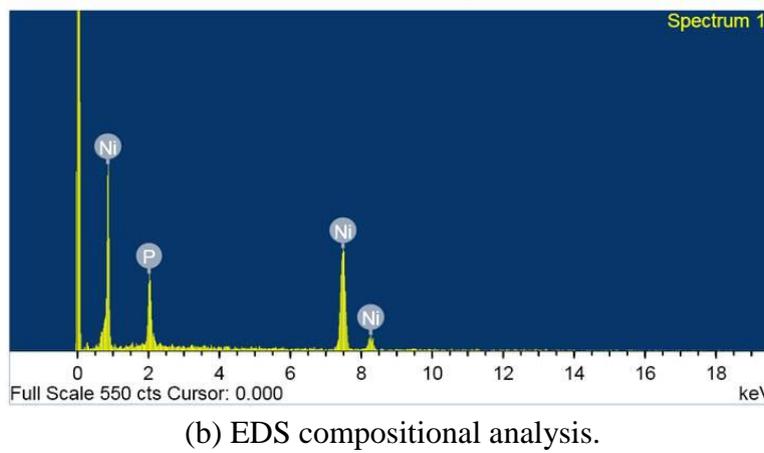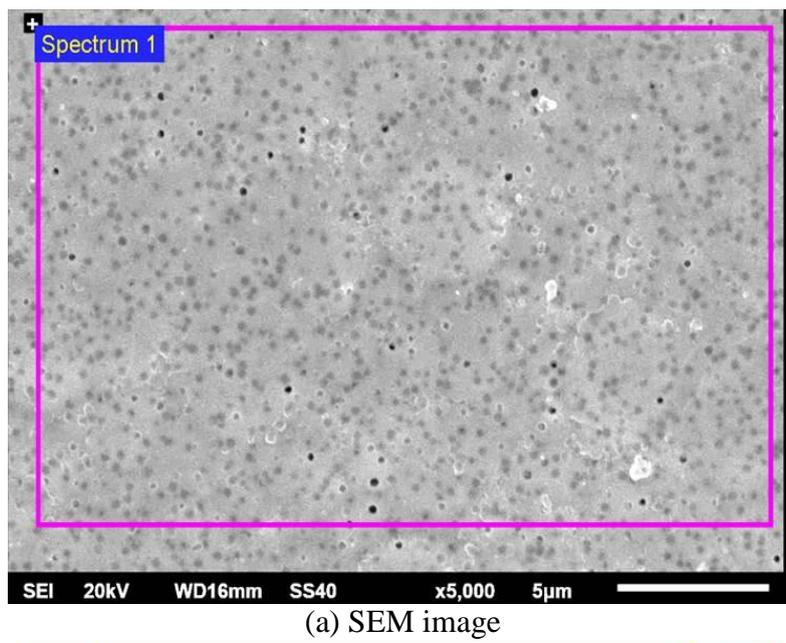
Figure 5. Characterized 5052 aluminun surface subjected to Ni-P-PTFE electroless coating.

3.2 Contact angle

The surface energy of the coated layer is observed by a contact angle measurement SD120D (IVTECH Inc).

Left Angle : 72.3
Center Angle : 72.1
Right Angle : 71.9

(a)Ni–P

Left Angle : 103.5
Center Angle : 103.4
Right Angle : 103.4

(b) Ni-P-PTFE
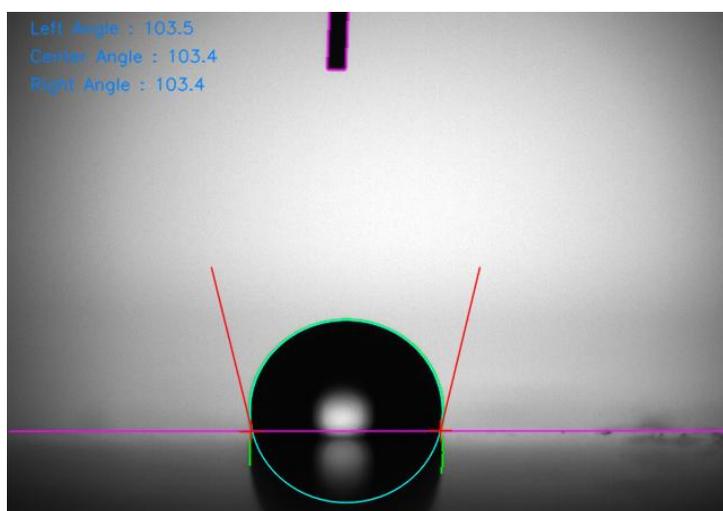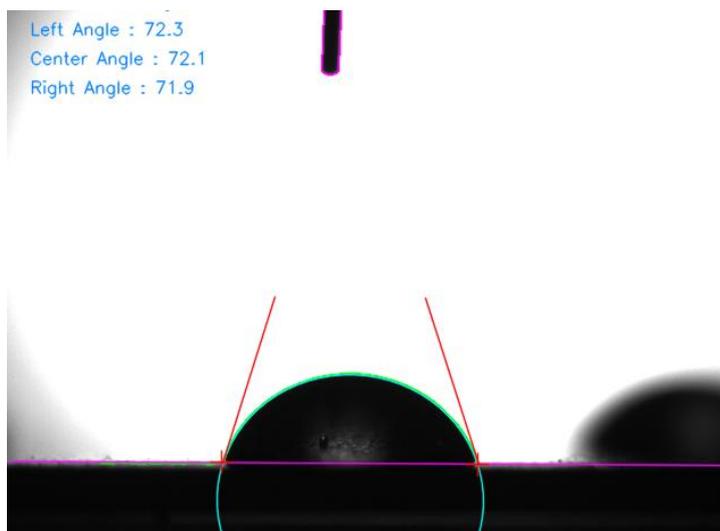
Figure 6. Drop of water on the coating layer in sessile drop measurement of contact angle.

The surface to the water product in the PEMFC behaves as a membrane under tension. Surface tension arises due to the attractive force between water molecules. The contact angle was caused by the equilibrium within liquid, solid and air interfaces. Hence, the hydrophobic surface enhances the whole behaviour on the solid interface as shown in Fig. 6. As the contact angle with water, the Ni-P and Ni-P-PTFE composite coated layers are 72° and 103°, respectively. The result was consistent to the previous conclusion that distributed PTFE particles enhance hydrophobic character on the solid interface [19, 22]. The flooding phenomenon in the PEMFC is attributed to the redundant water in flow channel.

Hence, the extreme hydrophilic property deteriorates the mass transfer mechanism of reactant gas. The surface wettability of the bipolar plate is a crucial factor to PEMFC performance, and water production should be immediately removed to avoid flooding within the cathode side [21, 26-27]. The hydrophobicity of Ni element is attributed to the higher electronegativity of oxygen on the bulk surface [28]. Consequently, the result presented here demonstrated an involvement of Ni-P-PTFE coating with extreme low surface energy, which is beneficial to the mass-transfer phenomenon and enhances the removal of redundant water.

3.3 Corrosion resistance

Potentiodynamic polarization was employed to analyze the corrosion resistance of 5052 aluminum sheet in a simulated environment (0.5 M H_2SO_4 with 2 ppm HF solution) [29]. The potentiodynamic polarization curve depends on the rate of redox reaction on specimen. As the presented Tafel test, the corrosion current density values of these 5052 aluminum BPPs were 1.02×10^{-6}, 8.72×10^{-5} and 9.22×10^{-4} A/cm^2, respectively. The conductive Ni coating layer exhibits the superior corrosion resistance than substrate as the previous literature [14, 30]. The corrosion current of the 5052 aluminum sheet with a Ni-P-PTFE coating is one order of magnitude lower than the bare one as shown in Fig. 7. The corrosion resistance of 5052 aluminum sheet increased in the order substrate < Ni-P < Ni-P-PTFE, due to higher surface film resistance. The result corresponds to section 3.1 that the content of phosphorus is a crucial factor to against the corrosive behaviour. Consequently, the lower corrosion potential and current density appears on the Ni-P-PTFE curve. The deviation of Tafel curve is consistent with electrochemical mechanism that the electron acceptor and donor reactions at the solution/bulk interface changed with the coated layer.
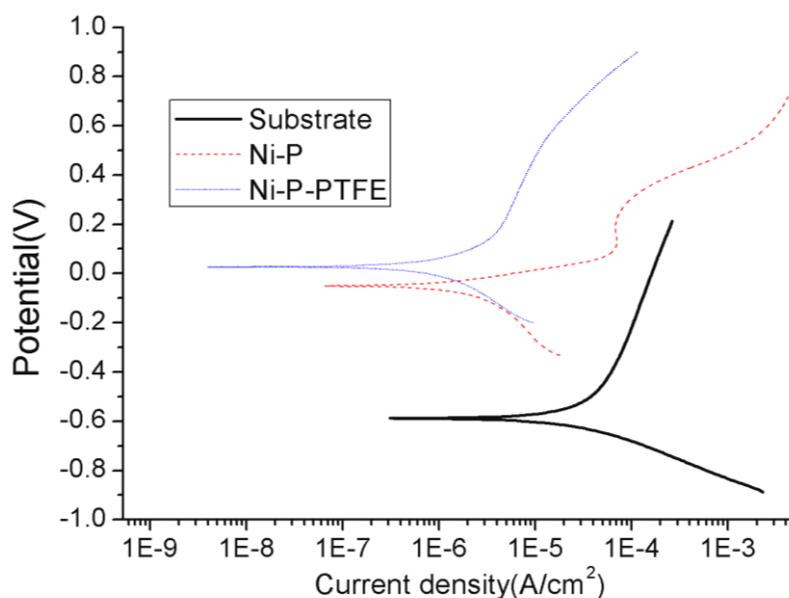
Figure 7. Polarization curves of 5052 aluminum with and without the coating in a solution (0.5 M H_2SO_4 + 2 ppm HF solution). The scanning rate was 0.166m V/sec at room temperature.

3.4 Interfacial contact resistance

The contact resistance versus compaction force curves of coated 5052 aluminum sheet are shown as Fig. 8. In the interfacial resistance measurement, the total resistance contains bulk materials and auxiliary components as in Section 2.3. Furthermore, the bulk resistance also depends on the chemical composition, roughness and geometry of its surface [30]. The contact resistance for the coated 5052 aluminum sheet decreased significantly with increasing compaction force (20-150 N/cm^2). The trend instantly approximated to stable field when the compaction pressure is above 150 N/cm^2. The result indicated that the surface contact resistance decreased significantly with the 5052 aluminum sheet coated with Ni-P-PTFE compared with the Ni-P as Fig. 8. The surface contact resistance for different materials is in the order of Ni-P-PTFE > Ni-P. As the curve tendency, the passive layer (oxide film) and PTFE particles reduces the electrical conductivity of 5052 aluminum sheet which subjected to the Ni-P-PTFE coating. It is reasonable that the small contact resistance benefits to the whole PEMFC performance [31], but the excessive force results in the damage of carbon paper and membrane. The measured contact resistance values were 18.5 mΩ · cm^2 (Ni-P-PTFE) and 13.2 mΩ · cm^2 (Ni-P-PTFE) at the same compaction force (200 N/cm^2) . Hence, the compaction force value was loaded as 200 N/cm^2 for the PEMFC. Summarily, the differences in the interfacial contact resistance condition related to the nickel element and PTFE particles of the coating, resulting in the superior performance for Ni-P coating [19, 30].
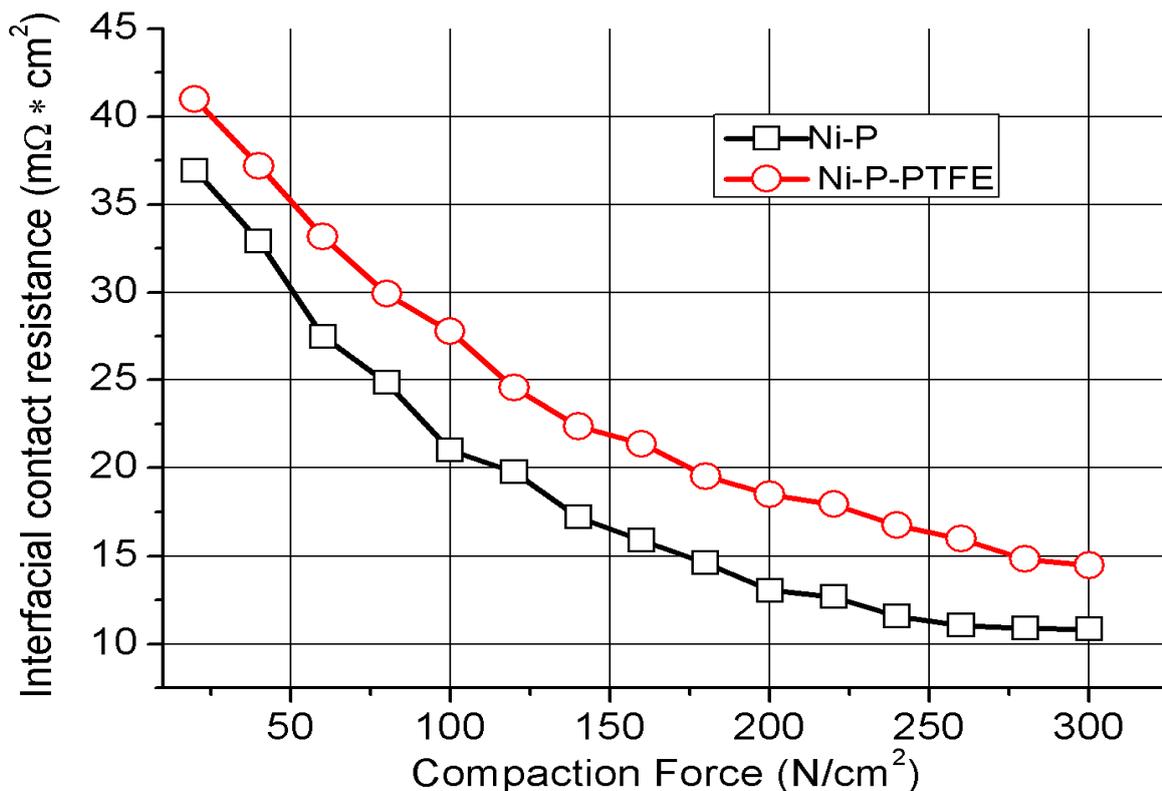
Figure 8. Comparison of contact resistance for Ni-P and Ni-P-PTFE coated bipolar plates.

3.5 Assembly test

The whole PEMFC performance using various modifications (substrate, Ni-P and Ni-P-PTFE) on the bipolar plate is shown in Fig. 9. The substrate exhibits inferior performance due to the oxide film formed on the sheet surface after the performance test. The Ni-P coating with superior electric conductivity was discussed in Section 3.4 and demonstrates the superior performance in the ohmic loss region (50-600 mA/cm^2) [24]. However, rapid electrochemical reaction occurs above a current density 600 mA/cm^2, which enhances the abundant water accumulation in the flow field. The error bar is represented as the error value (5%) in this experiment. Hence, the Ni-P-PTFE coating demonstrates superior performance in the concentration polarization region (600-1150 mA/cm^2), which the Ni-P-PTFE coating layer effectively removes the redundant water by its hydrophobic character.
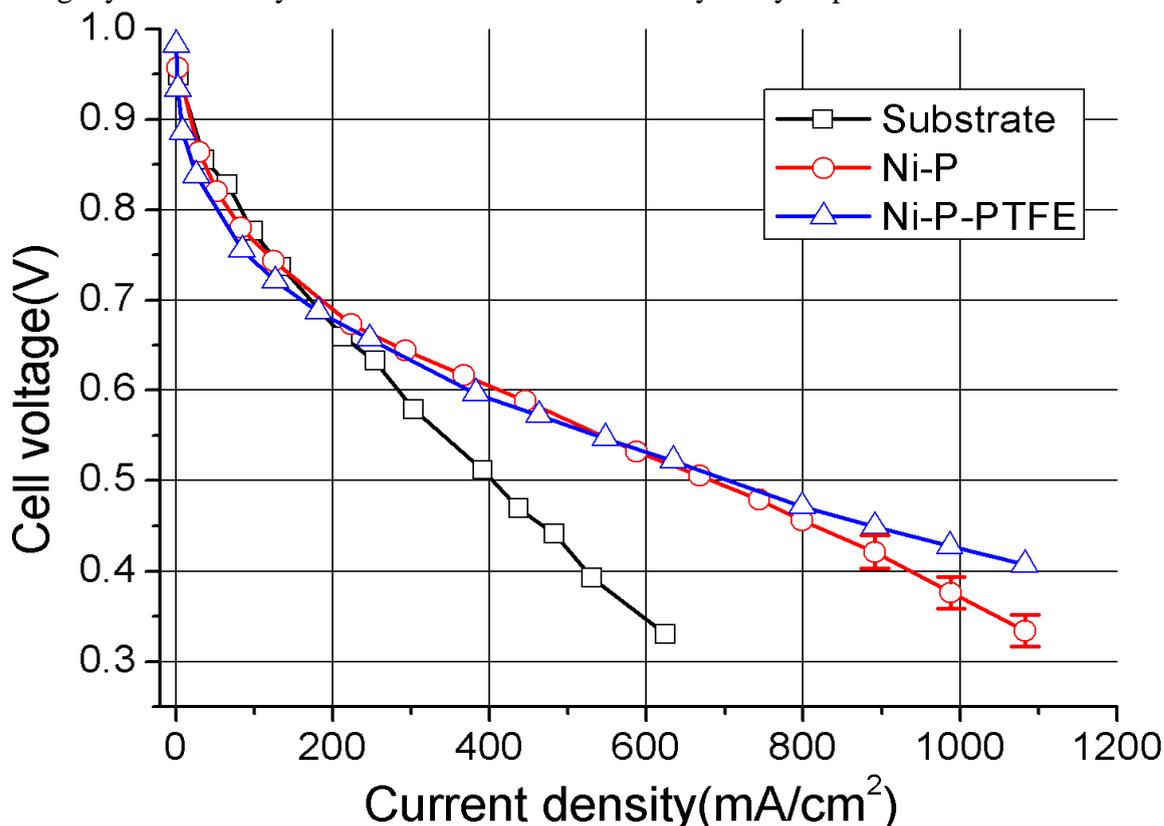
Figure 9. Performance comparisons of coated and bare 5052 aluminum bipolar plates. Cells of 25 cm^2 area were operated 70℃ with hydrogen and oxygen gas.

The moderate water enhances the electron conductivity in the membrane, but the redundant water causes two problems in the PEMFC. Firstly, the mass transfer mechanism is blocked due to the redundant water accumulated in the flow channel. Additionally, the metallic materials (inlet, outlet, bipolar plate and end plate) are seriously corroded by the excessive waster product. Since the water management is a crucial factor to bipolar plate, the active water management should be listed in the future demand to the PEMFC.

3.6 Corrosive behaviour of the metallic bipolar plate

The SEM micrograph of bipolar plate surface under the cathode condition for 50 hours is presented in Fig. 10. As the EDAX results, the oxide element on the Ni-P and Ni-P-PTFE surface are 36.5% and 16.8%, respectively. It is evident from Fig. 10(a) that the serious corrosion concave formed on the Ni- P coating surface resulting from water product. Additionally, the pinhole on the Ni-P-PTFE coating layer contrasts sharply with the corrosion phenomenon on the pure Ni-P coating. The hydrophobic material as demonstrated by Ni element to reduce the corrosive rate within the PEMFC [14, 30, 32].
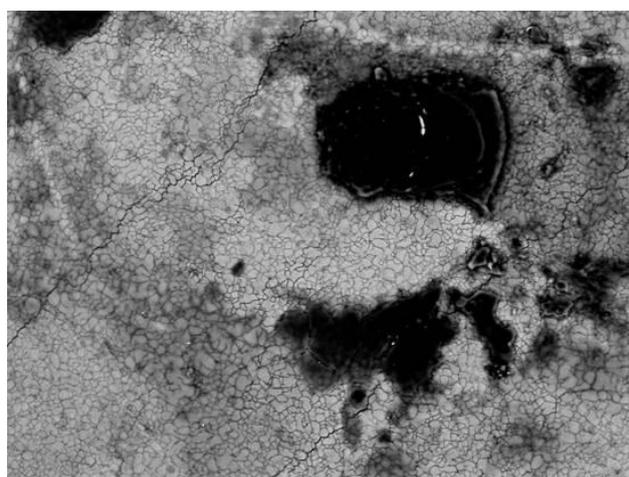
(a) Ni-P
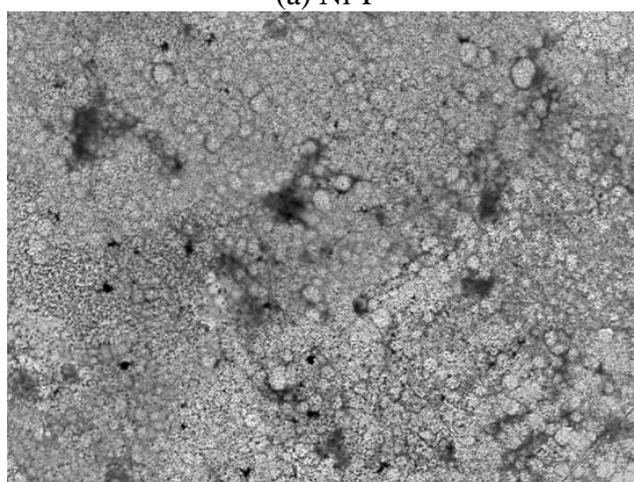
(b) Ni-P-PTFE

Figure 10. SEM images showing the corrosion behaviour that formed on the 5052 aluminum after 50 hours durability test in cathode side. The reactant gas temperature and compaction force were 70℃ and 200 N/cm^2, respectively.

Hence, the corrosion behaviour strongly related to the water product in flow channel, and the variant from unity is attributed to the physical property on the surface treatment. This conclusion corresponds to the Tafel and contact angle measurement as above, so the surface modification enhances the whole performance of PEMFC. Summarily, the active water management benefits to the whole performance of PEMFC [32], and the improvement of corrosion resistance by Ni-P-PTFE coating is proved at the present study. This mechanism successfully removes the excess water from the cathode side, and it decreases the corrosion rate of the bulk.

4. CONCLUSIONS

The active water management on the metallic polar plate is a crucial issue at present study. Within the PEMFC, the redundant water in the flow channel blocked the fuel gas transfer and corroded metallic component. Since the Ni-P-PTFE coating exhibits hydrophobic behaviour (contact angle =103°), so it successfully removes the excessive water in the cathode side. Furthermore, the corrosion current in the 5052 aluminum sheet subjected to the Ni-P-PTFE coating may be as much as one order of magnitude less than seen in the substrate. Finally, the implement of 5052 aluminum bipolar plate is proved after a period of the assembly test (50 hours). The PEMFC environment resulted in the serious corrosion behaviour with passive film on the Ni-P surface, and the passive film associated with the interfacial contact resistance. Furthermore, the oxide film increases the interfacial contact resistance and encumbers the overall performance. The Ni-P-PTFE coating is a promising candidate coating due to the superior corrosion resistance and hydrophobic character. The coating technique for bipolar plate is crucial to the durability and performance of PEMFC stack. Hence, it will be a promising substitute for the traditional bipolar plate at the near future.

References

1. C. Moisés Bautista Rodríguez, M. G. Araceli Rosas Paleta, J. Antonio Rivera Marquez, A. Belén Tapia Pachuca and J. Roberto García de la Vega, *Int. J. Electrochem. Sci.*, 4 (2009) 1754.
2. Y. C. Chen, K. H. Hou, C. H. Lin, C. Y. Bai, N. W. Pud and M. D. Ger, *J. Power Sources*, 197 (2012) 161.
3. B. Lee, K. Park and H. M. Kim, *Int. J. Electrochem. Sci.*, 8 (2013) 235.
4. C. Guzmán, A. Alvarez, S. Rivas, S. M. Durón–Torres, A.U. Chávez-Ramírez, J. Ledesma–Garcia and L.G. Arriaga, *Int. J. Electrochem. Sci.*, 8 (2013) 8893.
5. I. Dedigama, K. Ayers, P. R. Shearing and D. J. Brett, *Int. J. Electrochem. Sci.*, 9 (2014) 2662.
6. C. Y. Lee, S. J. Lee, Y. M. Lo and Y. M. Liu, *Int. J. Electrochem. Sci.*, 9 (2014) 272.
7. H. Guilin, Y. Xu and Z. Zhang, *Int. J. Electrochem. Sci.*, 9 (2014) 1902.
8. H. Su, C. Sita and S. Pasupathi, *Int. J. Electrochem. Sci.*, 11 (2016) 2919.
9. P. L. Hentall, J. B. Lakeman, G. O. Mepsted, P. L. Adcock, and J. M. Moore, *J. Power Sources*, 80 (1999) 235.
10. A. Miyazawa, E. Tada and A. Nishikata, *J. Power Sources*, 231 (2013) 226.
11. M. R. Belmonte, J. T. Pérez-Quiroz, J. Terán-Guillén, J. Porcayo-Calderón, A. Torres-Acosta and G. Orozco-Gamboa, *Int. J. Electrochem. Sci.*, 7 (2012) 1079.
12. L. C. Tsai, H. H. Sheu, C. C. Chen and M. D. Ger, *Int. J. Electrochem. Sci.*, 10 (2015) 317.
13. H. H. Sheu, C. H. Lin, S. Y. Jian, H. B. Lee, B. R. Yang and M. D. Ger, *Int. J. Electrochem. Sci.*, 11 (2016) 7099.

14. A. E. Fetohi, R. M. Abdel-Hameed, K. M. El-Khatib and E. R. Souaya, *Int. J. Hydrogen Energ.*, 37 (2012) 7677.
15. H. Husby, O. E. Kongstein, A. Oedegaard and F. Seland, *Int. J. Hydrogen Energ.*, 39 (2014) 951.
16. W. M. Yan, H. S. Chu, Y. L. Liu, F. Chen and J. H. Jang, *J. Power Sources*, 36 (2011) 5435.
17. C. Y. Lee, C. Y. Chao and C. L. Hsieh, *Int. J. Green Energy*, 9 (2012) 121.
18. C. H. Lin and S. Y. Tsai, *Appl. Energ.*, 100 (2012) 87.
19. Y. Fu, M. Hou, H. Xu, Z. Hou, P. Ming, Z. Shao and B. Yi, *J. Power Sources*, 182 (2008)580.
20. S. J. Lee, C. Y. Lee, K. T. Yang, Y. M. Lee, Y. J. Chang and C. L. Ho, *Int. J. Green Energy,* 10 (2013) 739.
21. F. San, I. Isik-Gulsac and O. Okur, *Energy,* 55 (2013) 1067.
22. M. S. Ismail, D. B. Ingham, L. Ma and M. Pourkashanian, *Renew. Energ.,* 52 (2013) 40.
23. C. H. Lin, *Appl. Energ.,* 104 (2013) 898.
24. S. Y. Tsai, C. Y. Bai, C. H. Lin, G. N. Shi, K. H. Hou, Y. M. Liu and M. D. Ger, *J. Power Sources*, 214 (2012) 51.
25. T. Y. Chiang, A. Su, L. C. Tsai, H. B. Lee, C. Y. Lin, H. H. Sheu and C. C. Chang, *Int. J. Electrochem. Sci.*, 10 (2015) 1926.
26. S. Y. Tsai, C. H. Lin, Y. J. Jian, K. H. Hou and M. D. Ger, *Surf. Coat. Tech.*, 313 (2017) 151.
27. M. Dadfar, M. Salehi, M.A. Golozar and S. Trasatti, *Int. J. Hydrogen Energ.,* 41 (2016) 21375.
28. H. Rashtchi, K. Raeissi, M. Shamanian, Y. Acevedo Gomez, C. Lagergren, R. Wrel Lindstrőm and V. Rajaei, *Fuel Cells*, 6 (2016) 784.
29. M. T. Lin, C. H. Wan, W. Wu, *Int. J. Electrochem. Sci.*, 9 (2014) 7832.
30. R. Wlodarczyk, D. Zasada, S. Morel and A. Kacprzak, *Int. J. Hydrogen Energ.,* 41 (2016) 17644.
31. C. E. Lu, J. L. Lee, H. H. Sheu, K. H. Hou, C. C. Tseng and M. D. Ger, *Int. J. Electrochem. Sci.*, 10 (2015) 5405.
32. J. Jin, D. Zheng, S. Han, J. Ma and Z. Zhu, *Int. J. Hydrogen Energ.,* 42 (2017) 1142.